RSC Advances

This article can be cited before page numbers have been issued, to do this please use: R. N. Goyal, P. Gupta and M. Oyama, *RSC Adv.*, 2015, DOI: 10.1039/C5RA22682A.

ROYAL SOCIETY OF CHEMISTRY

www.rsc.org/advances

View Article Online
DOI: 10.1039/C5RA22682A

Electrochemical investigations of 8-hydroxydeoxyguanosine and its determination at edge plane pyrolytic graphite electrode

Pankaj Gupta[a], Munetaka Oyama[b], Rajendra N Goyal[a]*

[a]Department of Chemistry, Indian Institute of Technology Roorkee, Roorkee -247667 (India)
[b]Department of Material Chemistry, Graduate School of Engineering, Kyoto University, Kyoto - 615- 8520, Japan
*E.Mail : rngcyfcy@iitr.ac.in, Tel: +91-1332-285794 (O) Fax: +91-1332-273560

Abstract

The electrochemical oxidation of 8-hydroxydeoxyguanosine (8-OHdG) has been studied at edge plane surface of pyrolytic graphite electrode (EPPGE) by cyclic sweep, square wave voltammetry, spectral studies, controlled potential electrolysis and related techniques. The oxidation of 8-OHdG occurred in a single well-defined peak over the entire pH range. The effect of pH revealed that the oxidation of 8-OHdG involved equal number of electrons and protons. The 8-OHdG exhibited linear calibration curve over a concentration range of 0.5-100 μM and the detection limit and sensitivity are found to be 28×10^{-9} M and 1.068 $\mu A \mu M^{-1}$ respectively. The kinetics of the decay of the UV-absorbing intermediate generated during oxidation has been studied and the decay has been found to follow first order kinetics having rate constant (k) in the range $\sim 2.5 \times 10^{-3}$ s^{-1}. The products of electrochemical oxidations have been characterized by using GC-MS studies. A tentative mechanism for the oxidation of 8-OHdG has also been suggested.

Keyword: 8-Hydroxydeoxyguanosine, Electrochemical oxidation, Pyrolytic graphite electrode, Cyclic voltammetry.

View Article Online
DOI: 10.1039/C5RA22682A

Introduction

8-Hydroxydeoxyguanosine (8-OHdG or 8-oxo-7,8-dihydro-2'-deoxyguanosine, I) is one of the oxidized nucleosides produced, when DNA is attacked by the reactive oxygen species, ultraviolet light, or genotoxic agents [1, 2]. The increased level of 8-OHdG has been found in the body fluids and tissues during an inflammatory conditions, in response to the production of reactive oxygen species (ROS). The production of 8-OHdG in the tissue DNA has been found to be a sensitive, stable and integral biomarker of oxidative stress and cancer [3, 4]. It has been reported that the elevated level of 8-OHdG accumulates in the breast, gastric tumors and renal cell in comparison to the surrounding tissues, which directly indicates the enhanced oxidative stress in the tumor tissues and can be related to the initiation of carcinogenesis. In agreement with this fact, cancer cell lines have been found to contain elevated level of oxidized damaged DNA, when compared with surrounding cell lines. The oxidized deoxyguanosine may lead to detrimental consequences like genetic mutations, cancer, thus unrepaired DNA lesions excised and replaced by DNA repair mechanism and excreted in urine. The urinary excretion of DNA-repair product 8-OHdG can be used for the quantitative assessment of oxidative DNA damage in the human system [1, 5-8]. Oxidative stress and ROS-induced elevations of 8-OHdG have also been claimed associated with the neurological diseases such as Parkinson's, Alzheimer's, Huntington's and numerous pathological processes including cardiovascular disease, rheumatoid arthritis, pancreatitis, chronic hepatitis and inflammatory bowel disease [9-11]. Several analytical methods such as coupled-column HPLC with electrochemical detection, capillary electrophoresis, gas chromatography-mass spectrometry (GC/MS), ^{32}P-postlabeling and ELISA have been used for the measurement of the oxidative DNA damage [12-17]. However, most of these methods are complicated, tedious and require time consuming derivatization, sample

View Article Online
DOI: 10.1039/C5RA22682A

preparation and extraction steps. An electroanalytical method bypass such complicated procedures and proved to be a simple, highly-sensitivity, cost effective, rapid, convenient and effective tool for the analysis of biomolecules in pharmaceutical formulations and human body fluids [18].

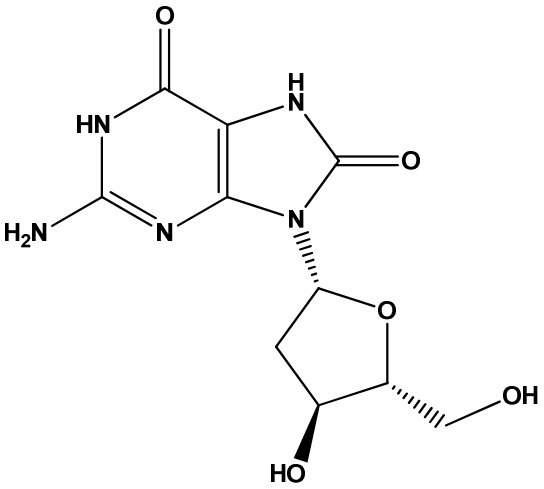

Structure of 8-OHdG (I)

In view of the importance of 8-OHdG as a specific marker of oxidative DNA damage, attempts have been made to determine this compound at variety of unmodified and modified electrodes. The determination of 8-OHdG have been extensively carried out and low detection limit for 8-OHdG is reported [19, 20]. Glassy carbon electrode (GCE) modified with nanocarbon film coupled with HPLC [21], poly (3-methylthiophene) [22, 23] and polyethylenimine [24] have been used for the determination of 8-OHdG. A review on the electrochemical devices for detection of DNA damage has also appeared in the literature [25]. A comparison of various methods reported in the literature is compiled in Table 1. The extensive literature survey indicates that several attempts have been focused to determine 8-OHdG, whereas, practically no attempt has been made to study the mechanism of electro-oxidation of 8-OHdG.

View Article Online
DOI: 10.1039/C5RA22682A

The main objective of the present work is to study the electrochemical oxidation of 8-OHdG at edge surface exposed pyrolytic graphite electrode. The kinetics of the UV-absorbing intermediate generated during electrochemical oxidation has been studied and the major oxidation products formed at physiological pH have been identified. A tentative mechanism for the oxidation of 8-OHdG has also been suggested.

2. Experimental

2.1. Instrumentation

Electrochemical experiments were performed using voltammetric analyzer (BAS, West Lafayette, USA) Epsilon EC-USB. All potentials are referred to Ag/AgCl (1M KCl) electrode at an ambient temperature, 25± 2 °C. Controlled potential electrolysis (CPE) for monitoring spectral changes was carried out by electrolyzing 0.1 mM 8-OHdG, in a single compartment cell equipped with three electrodes system using pyrolytic graphite plate (1 cm × 8 cm) as working, cylindrical platinum gauze as auxiliary and Ag/AgCl as reference electrode. The spectral changes during the electro-oxidation and the kinetic studies of the decomposition of the UV-absorbing intermediates generated during oxidation of 8-OHdG were performed using Shimadzu spectrophotometer (UV-vis) model UV-2450. Gas chromatography mass spectrometry (GC-MS) of the silylated samples were carried out by using Perkin-Elmer (model Clarus-500) mass spectrometer using helium as carrier gas at 30 ml/min. The glass column (1.8 m x 2.0 mm id.) containing 3% SE 30 on Chromosorb - W was used. Electron impact (EI) spectra were recorded at an electron beam voltage of 70 eV, whereas chemical ionization (CI) spectra were recorded using methane as the reagent gas at a pressure of $2x10^{-4}$ Torr. After injection the column was maintained at 100^{o}C for 10 min followed by an increase at a rate of 5^{o}C per minute. The pH

View Article Online
DOI: 10.1039/C5RA22682A

determination of buffer solutions was performed using Thermo Fisher Scientific, Singapore Digital pH meter (Eutech Instruments, model pH 700).

2.2. Chemicals

8-OHdG was purchased from Sigma-Aldrich (USA). Phosphate buffers of ionic strength (1.0 M) and appropriate pH were prepared from analytical grade chemicals (NaH_2PO_4 and Na_2HPO_4 from Merck) in double distilled water according to the method of Christian and Purdy [26]. Silylation grade acetonitrile (CH_3CN) and N,O-bis[trimethylsilyl]trifluotoacetamide (BSTFA) were incurred from Supelco, USA. The 2 mm × 2 mm × 10 mm pieces of pyrolytic graphite (PGE) obtained from Pfizer, USA as a gift were used for the fabrication of the electrode.

2.3. Preparation of sensor

The sensor was prepared according to the reported literature [27]. Briefly, a Pyrex glass tube of 80 mm length and 6 mm diameter was cleaned thoroughly and dried. An epoxy resin (Araldite, Ciba) was applied to the one end of the tube to fill in such a way so that tube is filled inside with epoxy to about 100 mm and then pyrolytic graphite piece ($10 \times 2 \times 2$ mm^3) was then slided from the open end of the tube with the help of a glass tube and pushed till it got covered with epoxy resin. Air pocketing was avoided in between the resin and the graphite piece inside the tube. After the resin had solidified, the glass tube end was rubbed on an emery paper gently (P-400) to expose the layered edge of the graphite piece. The electrode surface was then washed with distilled water several times in order to remove adhered fine carbon particles. A sufficient amount of mercury was then placed into the glass tube and a copper wire of appropriate length was inserted to make proper contact of the sensor to the outer circuit. To calculate the surface area of the exposed edge plane surface of the sensor, cyclic voltammograms (CVs) were recorded in the solution of 5 mM $K_3[Fe(CN)_6]$ at different scan rates using 0.1 mM KCl as the

View Article Online
DOI: 10.1039/C5RA22682A

supporting electrolyte. A redox couple was observed due to the Fe^{+2}/Fe^{+3}. The effective surface area was calculated from the slope of i_p vs. $\nu^{1/2}$ plot using Randles-Sevcik equation and found as 0.085 cm^2.

2.4 Procedure

The stock solution of 8-OHdG (1 mM) was prepared by dissolving the required amount in double distilled water. Working solutions were prepared by adding required volumes of the respective stock solution to 2.0 ml of phosphate buffer and the total volume was made to 4.0 ml with double distilled water. The voltammograms were then recorded after bubbling nitrogen for ~ 10 min. The surface of the electrode was cleaned after each run by rubbing it on an emery paper followed by washing with water. This procedure caused deviation in current, hence, the current reported are an average of at least three runs. The optimized parameters used for the square wave voltammetry were initial potential (E): 0 mV, final potential (E): 800 mV, square wave amplitude: 25 mV, potential step: 4 mV and square wave frequency (*f*): 15 Hz.

UV-vis spectral changes during the electro-oxidation of 8-OHdG were monitored in 200-400 nm region at a potential ~100 mV more positive than the peak potential. Throughout the electrolysis the solution in the working compartment was bubbled slowly with N_2 gas and stirred with a teflon-coated magnetic stirring bead. Nearly 3 mL of the electrolyzed solution was taken from the working compartment of the electrolysis cell at 2 min. time intervals and transferred to 1 cm^3 quartz cuvette and the spectrum was recorded. When the absorbance at λ_{max} reduced to about 50%, electrolysis was turned off and spectral changes were monitored at different times to detect the wavelength of the UV-vis absorbing intermediate generated during the oxidation.

For the product identification, about 8-10 mg of the compound was electrooxidized at a potential ~100 mV more positive than the oxidation peak potential in a buffer of pH 7.2. The ionic

View Article Online
DOI: 10.1039/C5RA22682A

strength of the buffer was kept at (0.05M) as phosphate interferes in the silylation procedure. The progress of the electrolysis was monitored by recording UV-spectrum at different time intervals. When the absorbance at λ_{max} reached to minimal (usually 24 h), the electrolysis was stopped and the electrolyzed solution was removed from the cell and filtered using Whatman filter paper 42, lyophilized and the resulting solid was analyzed by GC-MS.

2.5. Characterization of the oxidation product

In order to identify the products formed upon electrochemical oxidation of 8-OHdG, few μg of the lyophilized product was put in a silylation vial and 300 μL of acetonitrile and 300 μL of BSTFA were added. The vial was heated at 110 ºC in an oil bath for 30 min and then cooled. After cooling 5 μL of the solution was injected in GC-MS.

3. Results and discussions

3.1. Voltammetric studies

Cyclic voltammetry provides the information about the redox process of reaction. Thus, the cyclic voltammograms for 100 μM of 8-OHdG were recorded using edge plain exposed pyrolytic graphite electrode (EPPGE) at a sweep rate of 100 mV s^{-1}. At pH 7.2, a well-defined oxidation peak at Ep (390 mV) was observed, when the sweep was initiated in the positive direction. In the reverse sweep no reduction peak was observed which confirmed the irreversible oxidation of 8-OHdG. A typical cyclic voltammogram observed for the oxidation of 8-OHdG is presented in Fig. 1. To ascertain the nature of the electrode reaction, the scan rate effect on the electrochemical response was performed in the range 5-200 mV s^{-1}. The oxidation peak current of 8-OHdG was found to increase linearly with the increase in the scan rate over the range used and the dependence of the peak current on scan rate can be expressed by the following linear relationship:

View Article Online
DOI: 10.1039/C5RA22682A

$i_p = 0.0908\ [v] - 0.337$

having a correlation coefficient of 0.998, where v is the scan rate in mV s^{-1} and i_p is the peak current in μA. The linear relation between i_p versus scan rate (v) (inset of Fig. 1) indicated that oxidation of 8-OHdG at the EPPGs was adsorption controlled, which was further confirmed by the linearity of $i_p/v^{1/2}$ vs. log v and log i_p vs. log v plots. The following relation was observed for log i_p vs. log v plot:

$\log i_p = 1.0273 \log v - 0.1179$

having a correlation coefficient 0.999. The slope value (> 0.5) of log i_p vs. log v plot further suggested that 8-OHdG underwent an oxidation involving adsorption-controlled process at the surface of the EPPGE [28, 29].

As square wave voltammetry (SWV) is considered to be more sensitive, further studies on the oxidation peak of 8-OHdG, are carried out using SWV. The effect of the pH on the anodic peak potential of 8-OHdG was investigated using EPPGE. The peak potential of 8-OHdG was considerably influenced by the pH value of the supporting electrolyte. It was found that with the increasing pH in the range of 2.2–10.5, the oxidation peak potential of 8-OHdG shifted towards less positive potentials. The nature of Ep versus pH plot was linear and observed the linear regression equation-

E_p/mV (pH 2.2 – 10.5) = -60.30 pH + 791.06

with a correlation coefficient of 0.9975. The slope of 60.30 mV per pH of the plot indicated that the number of electrons and protons involved in the oxidation of 8-OHdG are equal [22, 30].

The dependence of the oxidation peak current (i_p) of 8-OHdG on square wave frequency (f) was also studied in the range of 5-40 Hz at pH 7.2. The oxidation peak current (i_p) of 8-OHdG was

View Article Online
DOI: 10.1039/C5RA22682A

found to increase linearly with increase in the square wave frequency and the linear relation between i_p and f can be expressed by the relation:

i_p (μA) = 0.9401[f] - 2.80

having a correlation coefficient of 0.999. The slop of the plot is in agreement with an adsorption controlled electrochemical process, which supports the inferences obtained from cyclic voltammetric studies [31].

The effect of the concentration of 8-OHdG on the oxidation peak current was examined at optimized parameters of SWV in the phosphate buffer of pH 7.2. Fig. 2 shows the square wave voltammograms observed for various concentration of 8-OHdG at the EPPGE. The peak current (i_p) was found to increase linearly with an increase in 8-OHdG concentration. The inset of Fig. 2 shows the corresponding calibration curve, demonstrating that in the range 1-100 μM, the anodic peak current has a good linear relationship with 8-OHdG concentration. The linear relationship between the oxidation peak current and concentration of 8-OHdG can be expressed by the relation:

i_p (μA) = 1.0688C (μM) + 4.1842

with a correlation coefficient of 0.994. The detection limit (LOD) and the limit of quantification (LOQ) were calculated by using the relation 3σ/b and 10σ/b and found to be 28 nM and 93 nM, respectively, where σ is the standard deviation of the blank solution and b is the slope of the calibration plot.

3.2. Spectrophotometric study

The UV-vis spectral changes during electrochemical oxidation of 8-OHdG were monitored at pH 7.2. A typical UV-spectrum of 8-OHdG exhibited two well defined absorption bands at λ_{max}=293 and 245 nm, (Fig. 3, curve 1). Upon application of a potential 100 mV more

View Article Online
DOI: 10.1039/C5RA22682A

positive than the peak potential of 8-OHdG, absorbance in the region 240-320 nm decreases systematically, whereas, the absorbance in the region 225-235 nm increase systematically (Fig. 3, curve 2-20). Curve 20 (in Fig. 3) was recorded after 40 min. of electrolysis and both the absorption peaks (293 nm and 245 nm) completely disappeared and a new band at 224 nm observed as shown in the inset of Fig 3. Thus, it is clear that the products of oxidation absorb at shorter wavelength in comparison to the starting material. A clear isosbestic band at 236 nm was observed during spectral changes.

The kinetics of the decomposition reaction of the UV-absorbing intermediate generated during electro-oxidation was monitored by recording absorbance at selected wavelengths. For this purpose, electro-oxidation was carried out and when the absorbance reached to about 50%, (corresponding to curve 5 in Fig. 3) the electrolysis was terminated and the decay of the absorbance at 245 nm and 293 nm were monitored as a function of time. The absorbance vs. time profile showed an exponential decay and the plots of log ($A-A_\infty$) vs. time were linear, indicating thereby that the decomposition reaction of the UV-absorbing intermediate followed first-order kinetics (Fig. 4). The values of the rate constants were calculated from the slope value of log ($A-A_\infty$) versus time plots and are presented in Table 2. The cyclic voltammograms was also recorded to monitor the progress of electrolysis of 8-OHdG at different times. At pH 7.2, when a potential ~100 mV more positive than anodic peak potential of 8-OHdG was applied, the peak current of 8-OHdG systematically decreased as shown in Fig. 5.

3.3. Product Characterization

The products of oxidation of 8-OHdG were characterized by recording GC-MS of the silylated lyophilized product. The total ion current chromatogram exhibited a major peak at 32.57 min together with small peak at 22.51, 23.90, 27.10, 28.52 and 28.60 min as shown in Fig.

View Article Online
DOI: 10.1039/C5RA22682A

6. The peak corresponding to 32.57 min exhibited a molar mass peak at 589 (M^+, 10.5%) and 574 (M^+-15, 2.0%). The molar mass of 589 corresponded to hexasilylated 5-guanidinoimidazolidine-2,4-dione as shown in Scheme 1.

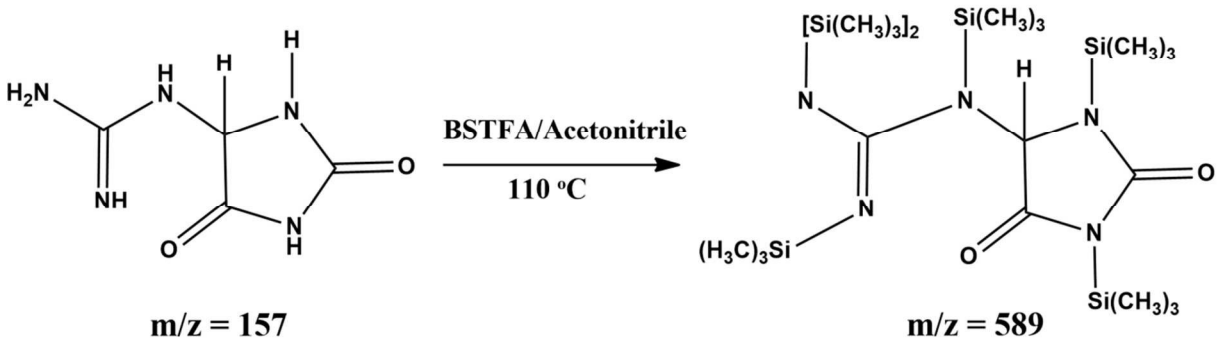

Scheme 1

The peak at Rt ~ 28.60 min exhibited molar mass of 517 and corresponded to penta silylated molecule of 5-guanidinoimidazolidine-2,4-dione. The formation of such imidazole derivative has also been observed during the electro-oxidation of guanosine [32-34]. Thus, it appears that during electro-oxidation the deoxyribose unit is hydrolyzed and removed from 8-OHdG.

The chemical ionization mass spectrum was then recorded to confirm the molar mass of 589 for the hexasilylated species using methane. In this case a peak at Rt ~ 33.67 min was observed in the chromatogram, which showed the molar mass at 590 (M^+ +1; 48.4%). Other major high mass peaks in the spectrum were observed at 574, (M^+ -CH_3; 100%); 618 (M^+ +C_2H_5; 4%); and 630 (M^+ +C_3H_7; 1%). Thus, it was confirmed that the major product of electro-oxidation had a molar mass of 157, which on silylation gave peak corresponding to 589 (M^+).

The formation of deoxyribose was also confirmed in the electrolyzed product of 8-OHdG. The small peak at 22.55 min in the GC-MS indicated a molar mass of 350 (M^+, 7.4%) as shown in Scheme 2.

View Article Online
DOI: 10.1039/C5RA22682A

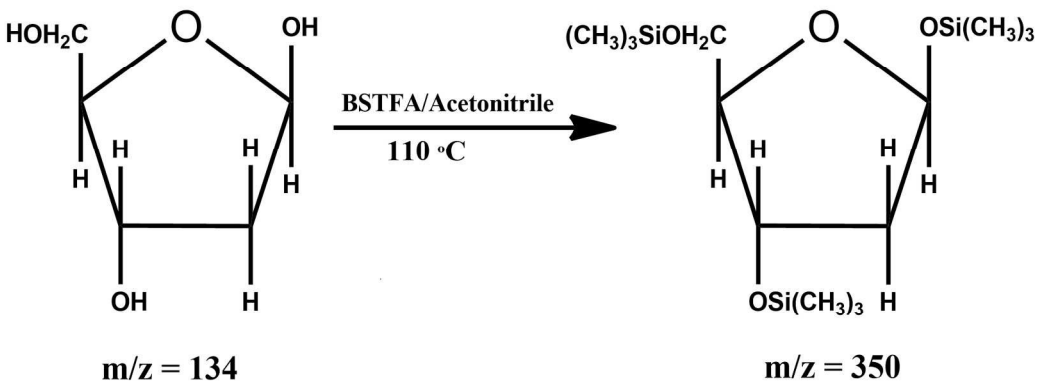

Scheme 2

The fragmentation pattern gave a clear M^+-15 peak at 335 (2.1%). Hence, it is concluded that deoxyribose unit is detached from 8-OHdG during electrooxidation. The hydrolysis of sugar moiety in purine nucleoside and nucleotides is common during oxidation and has been reported earlier [34, 35].

3.4 Coulometric Experiment

The experiment value of 'n', number of electrons involved in the oxidation of 8-OHdG was determined by plotting change in current with time. The resulting plot was exponential for the first 15-20 min of electrolysis, whereas, a significant deviation was observed after that. Hence, it was concluded that followup chemical reactions play a significant role after 15-20 min [36]. The value of 'n' calculated was found to be 1.8 ± 0.2 at pH 7.2. Thus, it seems reasonable to conclude that number of electrons involved in oxidation is ~ 2.0.

3.5 Reaction Mechanism

The observed results indicate that electrooxidation of 8-OHdG occurs in $2e^-$, $2H^+$ reaction, to give a UV-absorbing intermediate, which decompose in follow up chemical reactions to give 5-guanidinoimidazolidine-2,4-dione (IV) as a major product. Following tentative mechanism can be suggested for the electrooxidation of 8-OHdG. The first step of oxidation

View Article Online
DOI: 10.1039/C5RA22682A

involves $2e^-$, $2H^+$ oxidation of 8-OHdG to give diimine species (II). The diimine species (II) is readily attacked by water to give imine alcohol (III). The hydration of species II was first order reaction and the k values observed were 0.0025 s^{-1} and 0.0024 s^{-1} at pH 7.2. In a series of followup reactions imine alcohol (III) gives the major product 5-guanidinoimidazolidine-2,4-dione. The major steps involved in the oxidation are shown in **Scheme 3**. Similar steps for the oxidation of purines and their nucleosides are already reported in the literature [32, 37-39]. Thus, in contrast to adenosine and guanosine, where dimers or oligomers have been observed as products, the oxidation of 8-OHdG follows a simple path to give (IV) as the major product. One of the possible reasons for this difference in behavior may be the higher positive potential required for the oxidation of adenosine and guanosine in contrast to the less potential for 8-OHdG.

Conclusion

In this study, electrochemical oxidation of 8-OHdG in phosphate buffers has been studied by cyclic voltammetry and controlled potential electrolysis. The UV-vis spectral behaviour during oxidation has been studied using EPPGE. Electrochemical studies of 8-OHdG have provided significant information about its basic oxidation chemistry. The investigations clearly demonstrate that the electrochemical oxidation of 8-OHdG proceeds via a $2e^-$, $2H^+$ mechanism and it was found that the generated UV-absorbing intermediate (Scheme-1 (I)) decayed to follow first order kinetics. The major product of oxidation has been characterized as 5-guanidinoimidazolidine-2,4-dione (IV) by GC-MS. The suggested tentative mechanism was explained by all the observed voltammetric, coulometric and spectral behaviour. The detection limit for the 8-OHdG is found to be 28 nM. A comparison of the detection limit at other electrodes reported in recent literature is presented in Table 1 and indicates that the electrode is

View Article Online
DOI: 10.1039/C5RA22682A

satisfactory for the determination of 8-OHdG and no complicated modification of the electrode surface are needed to achieve similar order of detection limit. Thus, it is expected that the oxidation of 8-OHdG could serve as an important tool for the biochemists to deeply understand the medicinal applications of the products.

Acknowledgements

Thanks are due to the Japan Society for the Promotion of Science (JSPS) for awarding Invitation Fellowship for Research in Japan to RNG. One of the authors (PG) is thankful to the Ministry of Human Resource Development, New Delhi, for the award of Senior Research Fellowship.

View Article Online
DOI: 10.1039/C5RA22682A

References

1. S. Nishimura, *DNA Repair*, 2011, **10**, 1078-1083.
2. M. Dizdaroglu, P. Jaruga, M. Birincioglu and H. Rodriguez, *Free Radical Biol. Med.*, 2002, **32**, 1102-1115.
3. C.Y. Ock, E. H. Kim, D. J. Choi, H. J. Lee, K. B. Hahm and M. H. Chung, *World J Gastroenterol.*, 2012, **18**, 302-308.
4. A. Valavanidis, T. Vlachogianni and C. Fiotakis, *J. Environ. Sci. Health., Part C*, 2009, **27**, 120-139.
5. T. lida, A. Furuta, M. Kawashima, J. Nishida, Y. Nakabeppu, and T. Iwaki, *Neuro-Oncol.*, 2001, **3**, 73-81.
6. M. Dizda, *Mutat. Res.*, 2015, **763**, 212-245.
7. M. Dizdaroglu, *Cancer Lett.*, 2012, **327**, 26-47.
8. M. K. Shigenaga, C. J. Gimeno and B. N. Ames, *Proc. Natl. Acad. Sci. USA*, 1989, **86**, 9697-9701.
9. R. Arunachalam, A. P. Reshma, V. Rajeev, S. B. Kurra, M. R. J. Prince and N. Syam, *The Saudi J Dent Res*, 2015, **6**, 15-20.
10. L. J. Kroese and P. G. Scheffer, *Curr Atheroscler Rep.*, 2014, **16:452**, 1-8.
11. G. G. Romanillos **US 8,389,005 B2** (2013).
12. H. Kasai, P. Svoboda, S. Yamasaki and K. Kawai*, Ind Health*, 2005, **43**, 333-336.
13. C. Tagesson, M. Kgllberg, C. Klintenberg and H. Starkhammar, *Eur J cancer*, 1995, **31A**, 934-940.
14. J. L. Ravanat, R. J. Turesky, E. Gremaud, L.J. Trudel and R. H. Stadler, *Chem. Res. Toxicol.*, 1995, **8**, 1039-1045.
15. S. Mei, Q. Yao, C. Wu and G. Xu, *J. Chromatogr. B*, 2005, **827**, 83-87.
16. V. L. Wilson, B. G. Taffe, P. G. Shields, A. C. Povey and C. C. Harris, *Environ. Health Perspect.*, 1993, **99**, 261-263.
17. B. Yin, R. M. Whyatt, F. P. Perera, M. C. Randall, T. B. Cooper and R. M. Santella, *Free Radical Biol. Med.*, 1995, **18**, 1023-1032.
18. R. N. Goyal and N. Jain, *Indian J. Chem.*, 2000, **39A**, 1222-1226.

View Article Online
DOI: 10.1039/C5RA22682A

19. C. Wan, T. Liu, S. Wei and S. Zhang, *Russ. J. Electrochem.*, 2008, **44**, 327-331.
20. A. Gutiérrez, S. Gutiérrez, G. García, L. Galicia and G. A. Rivas, *ECS Trans.,* 2010, **29**, 369-380.
21. D. Kato, M. Komoriya, K. Nakamoto, R. Kurita, S. Hirono and O. Niwa, *Anal. Sci.*, 2011, **27**, 703-707.
22. T. H. Li, W. L. Jia, H. S. Wang, R. M. Liu, *Biosens. Bioelectron.*, 2007, **22**, 1245-1250.
23. W. Yanhuai, L. Jing, L. Yan, M. R., Jiawenli, C.hui and W. Huaisheng, *Sci. China, Ser. B*, 2009, **52**, 2006-2012.
24. A. Gutiérrez, S. Gutiérrez, G. García, L. Galicia and G. A. Rivas, *Electroanalysis*, 2011, **23**, 1221-1228.
25. V. C. diculescu, A. M. C. Paquim and A. M. O. Brett, *Sensors*, 2005, **5**, 377-393.
26. G. D. Christian and W. C. Purdy, *J Electroanal. Chem.*, 1962, **3**, 363-397.
27. P. Gupta and R. N. Goyal, *J. Electrochem. Soc.,* 2014, **161 (4)**, H255-H259.
28. S. K. Yadav, B. Agrawal and R. N. Goyal, *Talanta*, 2013, **108**, 30-37.
29. P. Gupta and R. N. Goyal, *Electrochim.Acta*, 2015, **151**, 1-7.
30. X. Sun, L. Zhang, H. Zhang, H. Qian, J. Ji, L. Tang, Z. Li and G. Zhang, *Anal. Methods*, 2015, **7**, 6664-6671.
31. P. Gupta and R. N. Goyal, *RSC Adv.*, 2015, **5**, 40444-40454.
32. G. Dryhurst and G. F. Pace, *J. Electrochem. Soc.*, 1970, **117**, 1259-1264.
33. W. Luo, J. G. Muller, E. M. Rachlin, and C. J. Burrows, *Chem. Res. Toxicol.*, 2001, **14**, 927-938.
34. R. N. Goyal, N. Jain and D. K. Garg, *Bioelectrochem. Bioenerg.*, 1997, **43**, 105-114.
35. R. N. Goyal and G. Dryhurst, *J. Electroanal. Chem.,* 1982, **135**, 75-91.
36. G. Cauqis and V.D. parker, *in Organic electrochemistry*, ed. M.M. baizer, M. Dekker, 1973, p. 134, NewYork.
37. G. Dryhurst, Electrochemistry of biological molecules, *Academics Press,* 1977, 272-317.
38. Q. Li, C. B. McAuley and R. G. Compton, *J. Phys. Chem. B*, 2010, **114**, 7423-7428.
39. E. G. Fernandez, N. Alvarez, M. J. Castanon, A. J. M. Ordieres and P. T. Blanco, *Electroanalysis*, 2008, **20**, 833-839.

View Article Online
DOI: 10.1039/C5RA22682A

Figure Caption

Fig. 1: Typical cyclic voltammograms Observed for 100 μM 8-OHdG at scan rate 100 mV s^{-1} in phosphate buffer of pH 7.2 at pyrolytic graphite electrode. Inset is showing the graph between i_p and v. The background is shown by the dotted line.

Fig. 2: Square wave voltammograms observed for increasing concentration of 8-OHdG. Curves were recorded at (a) 0.5; (b) 2; (c) 5; (d) 10; (e) 20; (f) 30; (g) 50; (h) 80μM; (i) 100 μM using EPPGE in phosphate buffer of pH 7.2. The background curve is shown by dotted line. The observed calibration plot for 8-OHdG is shown in the inset.

Fig. 3: Spectral changes observed at pH 7.2 for electrooxidation of 0.2 mM 8-OHdG at an interval of 2 min each after application of 0.5 V vs. SCE. Inset is showing a comparison of 1st and 20th curves observed during spectral changes.

Fig. 4: Plot of the absorbance vs. time and log (A− A∞) vs. time (inset) plot observed at pH 7.2 at 245 nm for 8-OHdG.

Fig. 5: Cyclic voltammograms recorded for 100 μM 8-OHdG at pH 7.2. Curves were recorded at (1) 0; (2) 15; (3) 25; (4) 35; (5) 50; (6) 65; (7) 80; (8) 35; (9) 100; (10) 110; (11) 120 and (12) 130 min of electrolysis.

Fig. 6: Total ion current chromatogram obtained for the silylated oxidation products of 8-OHdG.

View Article Online
DOI: 10.1039/C5RA22682A

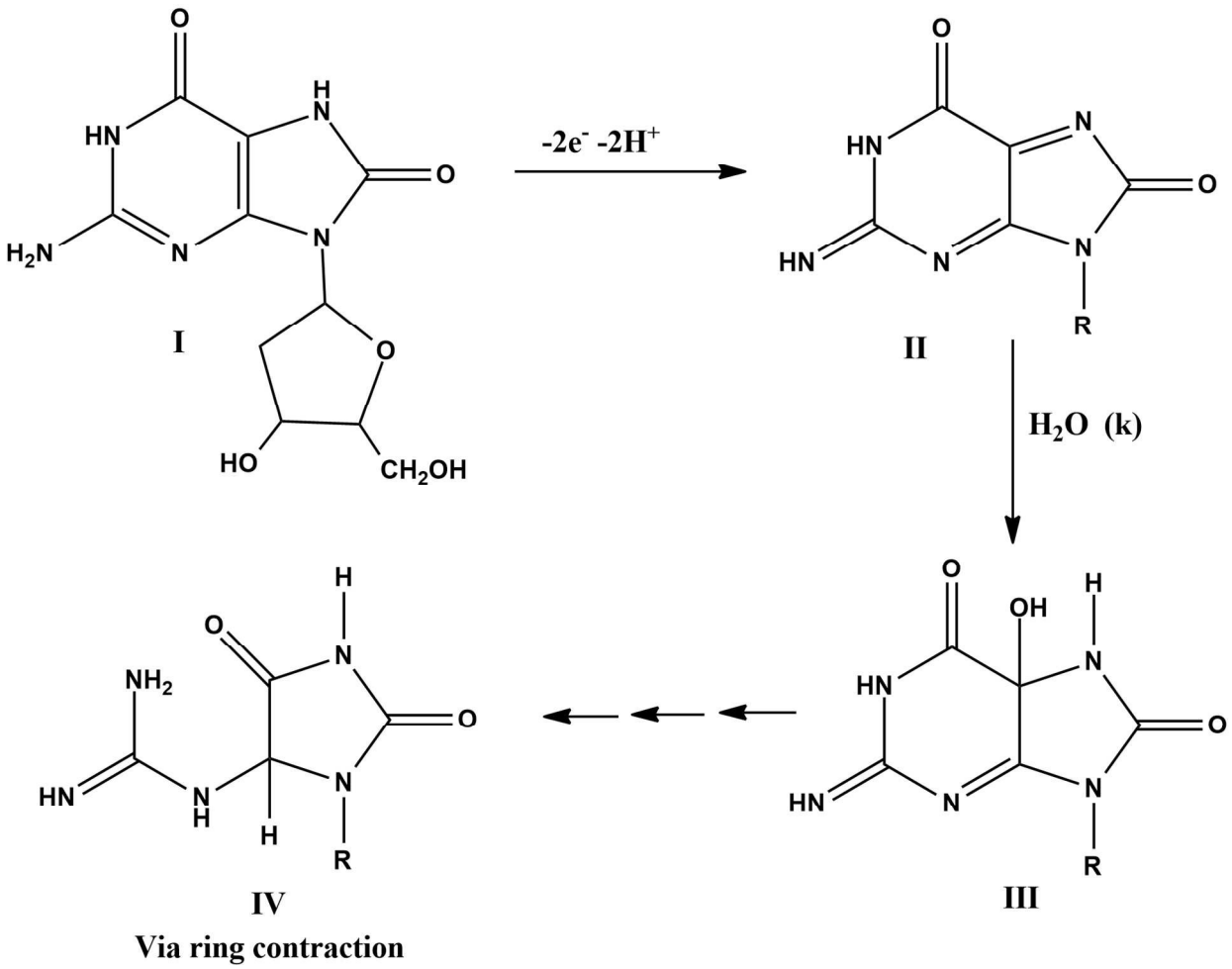

Scheme 3: Tentative reaction mechanism proposed for the electrooxidation of 8-OHdG.

View Article Online
DOI: 10.1039/C5RA22682A

Table 1: A comparison of the EPPGE with recently reported methods for the determination of 8-OHdG.

Sr. No.	Electrode Type	Linear range	Detection Limit	Reference
1	MWNT/GCE	0.08-5 µM	9 nM	19
2	GCE/CNT-Pnaf	0.5-20 µM	13 nM	20
3	Nano-carbon/GCE	0.02-0.5 µM	3 nM	21
4	poly(3-methylthiophene)/GCE	0.7-70 µM	100 nM	22
5	DNA/P3MT/GCE.	0.28-19.6 µM	56 nM	23
6	GCE/CNT-PEI	0.5-30 µM	100 nM	24
7	EPPGE	0.5-100 µM	28 nM	This work

*GCE- Glassy carbon electrode, MWNT- multi-wall carbon nanotube, Pnaf- poly-nafion, P3MT- poly(3-methylthiophene), PEI- polyethylenimine.

Table 2: Rate constant *(k)* values observed for the decomposition of UV absorbing generated intermediate during electrochemical oxidation of 8-OHdG at pH 7.2.

pH	λ_{max} (nM)	Rate (k×10−3 s−1)[a]
		Electrochemical
7.2	293	2.4
	245	2.5

[a] Average of at least three replicate determinations.

View Article Online
DOI: 10.1039/C5RA22682A

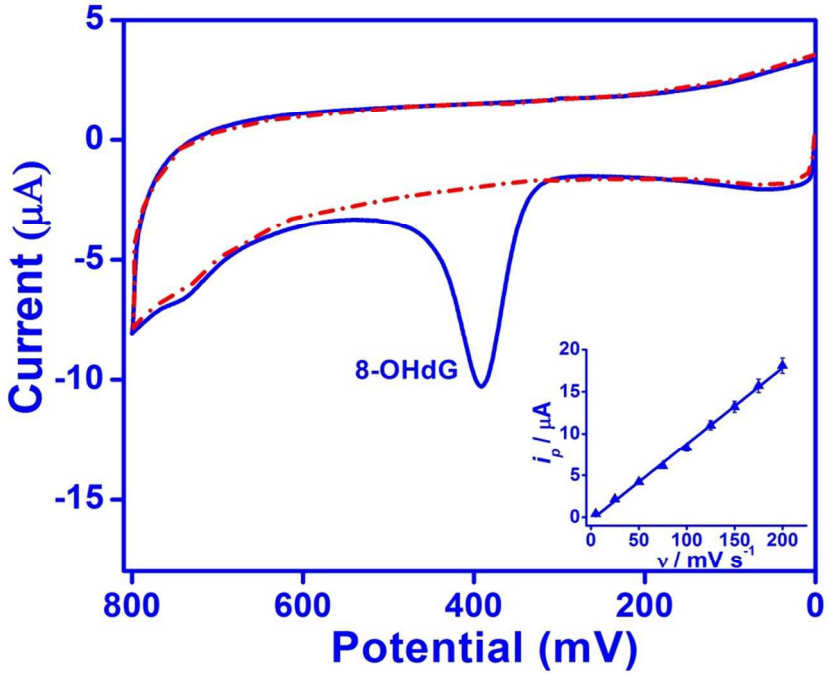

Fig. 1

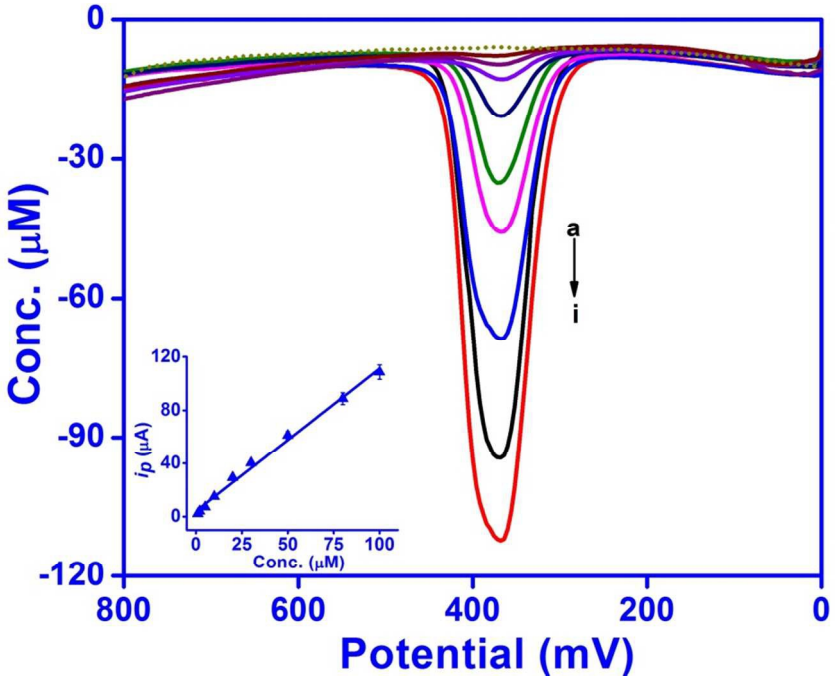

Fig. 2

View Article Online
DOI: 10.1039/C5RA22682A

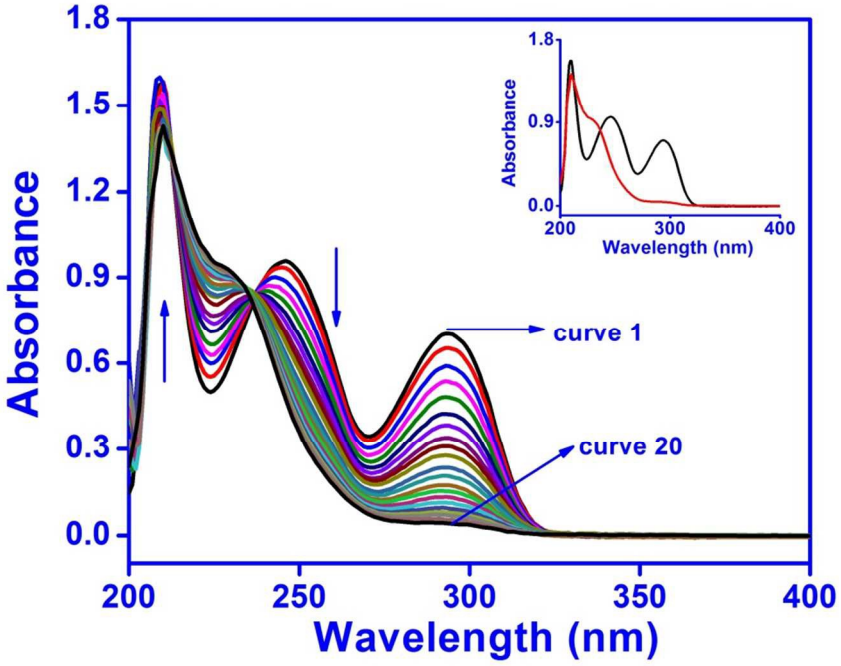

Fig. 3

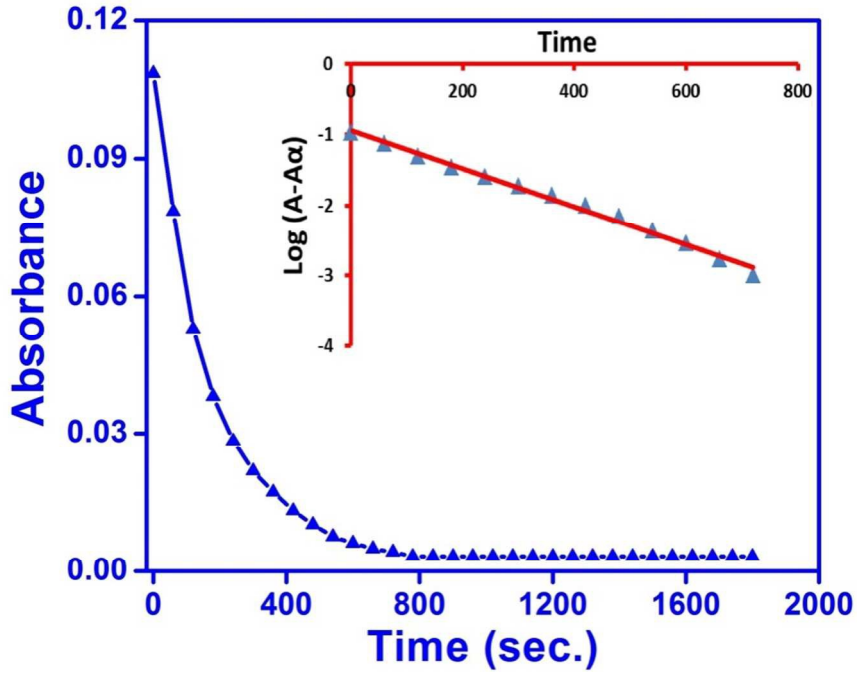

Fig. 4

View Article Online
DOI: 10.1039/C5RA22682A

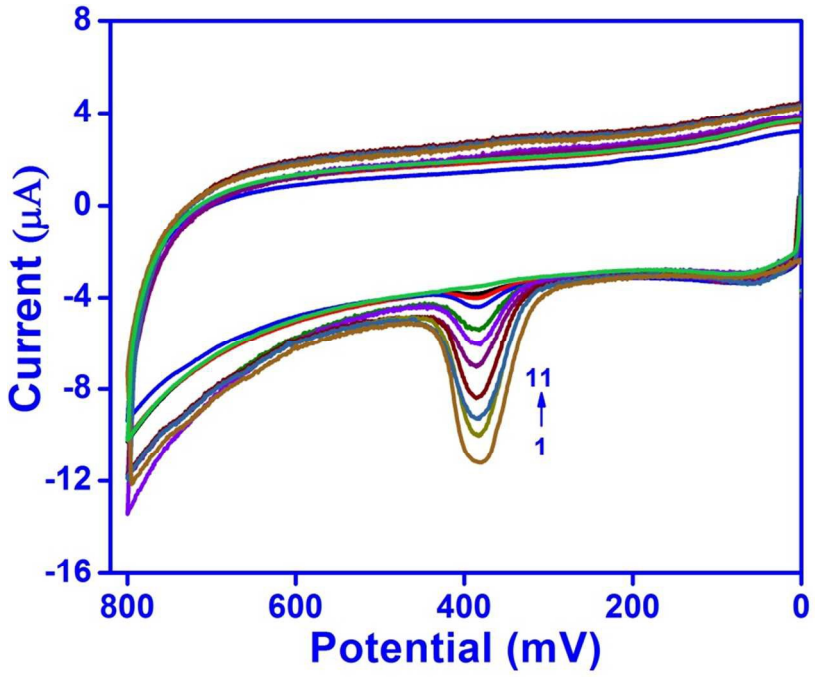

Fig. 5

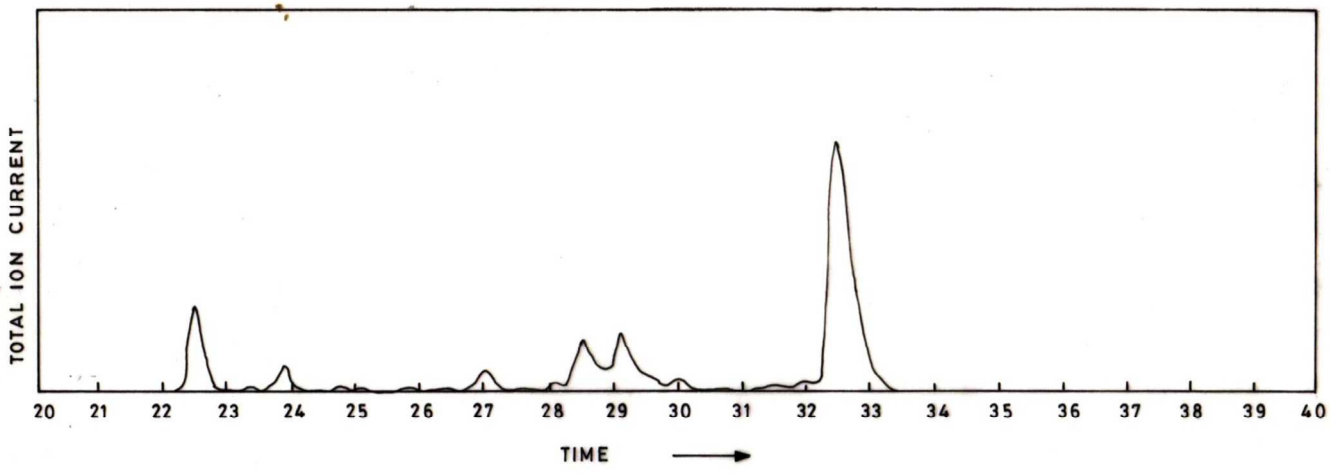

Fig. 6

View Article Online
DOI: 10.1039/C5RA22682A

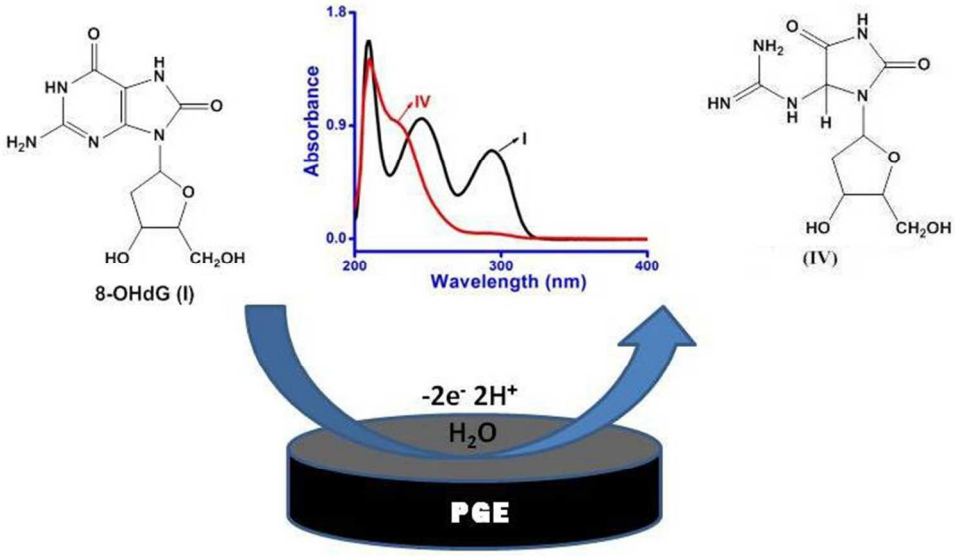

209x129mm (96 x 96 DPI)